

The climatic mass balance of Svalbard glaciers: a 10-year simulation with a coupled atmosphere - glacier mass balance model

K. S. Aas¹, T. Dunse¹, E. Collier², T. V. Schuler¹, T. K. Berntsen¹, J. Kohler³, B. Luks⁴

[1]{Department of Geosciences, University of Oslo, Oslo, Norway}

[2]{Climate System Research Group, Institute of Geography, Friedrich-Alexander University Erlangen-Nürnberg (FAU), Erlangen, Germany }

[3]{Norwegian Polar Institute, Tromsø, Norway}

[4]{Institute of Geophysics, Polish Academy of Sciences, Warsaw, Poland}

Correspondence to: K. S. Aas (k.s.aas@geo.uio.no)

Abstract

In this study we simulate the climatic mass balance of Svalbard glaciers with a coupled atmosphere-glacier model with 3-km grid spacing, from September 2003 to September 2013. We find a mean specific net mass balance of $-257 \text{ mm w.e. yr}^{-1}$, corresponding to a mean annual mass loss of about 8.7 Gt, with large interannual variability. Our results are compared with a comprehensive set of mass balance, meteorological and satellite measurements. Model temperature biases of 0.19 and $-1.9 \text{ }^\circ\text{C}$ are found at two glacier automatic weather station sites. Simulated climatic mass balance is mostly within about $100 \text{ mm w.e. yr}^{-1}$ of stake measurements, and simulated winter accumulation at the Austfonna ice cap shows mean absolute errors of 47 and $67 \text{ mm w.e. yr}^{-1}$ when compared to radar-derived values for the selected years 2004 and 2006. Comparison of modelled surface height changes from 2003 to 2008, and satellite altimetry reveals good agreement in both mean values and regional differences. The largest deviations from observations are found for winter accumulation at Hansbreen (up to around $1000 \text{ mm w.e. yr}^{-1}$), a site where sub-grid topography and wind redistribution of snow are important factors. Comparison with simulations using 9-km grid

1 spacing reveal considerable differences on regional and local scales. In addition, 3-km grid
2 spacing allows for a much more detailed comparison with observations than what is possible
3 with 9-km grid spacing. Further decreasing the grid spacing to 1 km appears to be less
4 significant, although in general precipitation amounts increase with resolution. Altogether, the
5 model compares well with observations and offers possibilities for studying glacier climatic
6 mass balance on Svalbard both historically as well as based on climate projections.

7

8 **1 Introduction**

9 The Svalbard archipelago has a glacierized area of ca. 34,000 km² (Nuth et al., 2013),
10 representing ~4 % of the world's land-ice mass outside the Greenland and Antarctic ice
11 sheets. If completely melted, the glaciers on Svalbard could potentially contribute to sea level
12 rise of 17 ± 2 mm sea level equivalent (SLE; Martin-Espanol et al., 2015). The archipelago
13 has already experienced significant warming during the 20th century (Førland et al., 2011)
14 and, with the expected retreat of the sea ice margin, further warming as well as precipitation
15 increases are expected (Day et al., 2012). Projections presented in the latest assessment report
16 of the IPCC (AR5) shows that annual-mean temperatures in this region could rise between 7
17 and 11 °C by the end of the 21st century under the RPC8.5 scenario, accompanied by a
18 projected precipitation increase between 20-50% (IPCC 2013). Svalbard glaciers are therefore
19 expected to undergo significant changes during this century (Day et al., 2012; Lang et al.,
20 2015a). However, reliable estimates of future glacier changes require modelling tools that are
21 able to reproduce recent observations. Current model estimates based on global climate
22 datasets (Marzeion et al., 2012; Marzeion et al., 2015) show significantly more negative mass
23 balance in this region than satellite altimetry and satellite gravimetry over the last decade
24 (Moholdt et al., 2010; Matsuo and Heki 2013).

25 Regional model estimates of surface mass balance of Svalbard glaciers have so far mainly
26 focused on individual or a few glaciers, and as noted by Lang et al. (2015b) typically been
27 based on empirical or statistical models. A number of dynamical downscaling simulations
28 focusing on Svalbard glaciers have been performed (Day et al., 2012; Claremar et al., 2012;
29 Lang et al., 2015a; Lang et al., 2015b). However, only two of these studies compare their
30 output with mass balance observations: Day et al. (2012; hereafter DA12) compares
31 precipitation from HadRM3 RCM (25-km grid spacing) with surface mass balance estimates
32 from Pinglot et al. (1999), and Lang et al. (2015b; hereafter LA15b) compares output from the

1 MAR model (10 km) to Pinglot et al. (1999, 2001) as well as a number of altimetry and
2 gravimetry studies of Svalbard glacier mass balance (Wouters et al., 2008; Moholdt et al.,
3 2010; Nuth et al., 2010; Mémin et al., 2011). Both studies show fair agreement with multi-
4 year accumulation records from Pinglot et al. (1999,2001). LA15b also finds mean elevation
5 changes in good agreement with satellite estimates, even though the differences are
6 substantial for some regions. However, DA12 and LA15b do not validate mass balance
7 estimates on time scales shorter than 4 years, nor do they validate on spatial scales that can
8 capture variations on individual glaciers. DA12 also suggests that a grid spacing of 1-5 km
9 may be needed to simulate surface mass balance in the complex terrain that is typical for
10 Svalbard.

11 In this study, we aim to i) simulate the climatic mass balance (CMB) of Svalbard glaciers
12 with a higher resolution than previously used with dynamical downscaling, ii) validate the
13 model with an extensive set of observations in this region, and iii) investigate the spatial
14 resolution needed to describe the observations. We apply a coupled atmosphere-glacier mass
15 balance model to the entire Svalbard region with a horizontal grid spacing of 3 km, thereby
16 capturing both regional averages for the period 2003-2013 as well as temporal and spatial
17 variations of individual glaciers. The results are validated with (i) observations from weather
18 stations, (ii) mass-balance stakes from four glaciers, (iii) snow accumulation across
19 Austfonna, measured by ground-penetrating radar (GPR), and (iv) satellite altimetry. To
20 examine the importance of model resolution in this region we also compare results from
21 domains with 9-km and 3-km grid spacing, and for a selected month, precipitation results
22 from 9-km, 3-km and 1-km grid spacing domains. Through this high-resolution simulation
23 and extensive model evaluation, we aim to provide a detailed estimate of recent CMB of
24 Svalbard glaciers, including its spatial and temporal variations.

25

26 **2 Methods**

27 In the following sections, we describe the two components of the coupled modelling system:
28 the Weather Research and Forecasting model (WRF; Sect. 2.1) and the CMB model (Sect.
29 2.2), including optimizations for high-Arctic conditions made in this study. In Sect. 2.3, we
30 describe the different validation data and sites before clarifying comparison methods in Sect.
31 2.4. Throughout this study we distinguish between the surface mass balance (SMB) and the
32 CMB as recommended by Cogley et al. (2011). The SMB specifies mass changes between the

1 surface and the last summer surface, whereas the CMB also accounts for internal
2 accumulation and ablation (i.e. below the last summer surface). We consider internal ablation
3 as negligible and it is therefore not explicitly treated in our application.

4 **2.1 The Weather Research and Forecasting model (WRF)**

5 The WRF model is a state-of-the-art mesoscale atmospheric model (Skamarock and Klemp,
6 2008) widely used for research and forecasting applications. In Svalbard, the model has been
7 used to study both atmospheric boundary layer processes (Kilpeläinen et al., 2011;
8 Kilpeläinen et al., 2012), and atmosphere–land surface interactions over both tundra (Aas et
9 al., 2015) and glaciers (Claremar et al., 2012), with horizontal grid spacing ranging from
10 several tens of kilometers to sub-kilometer scales. In this study, we use the advanced research
11 WRF version 3.6.1 configured with two nested domains of 9-km and 3-km horizontal grid
12 spacing. For a single month we also simulate the main regions of interest with additional
13 nested domains at 1-km. The WRF model setup and forcing strategy follows that of Aas et al.
14 (2015). The outer domain (9-km) covers a region of 1080 x 1080 km. As boundary conditions
15 for this domain we use the ERA-Interim reanalysis (Dee et al., 2011) with a 6-hour temporal
16 resolution. We employ the default boundary configuration in WRF, with the outermost grid-
17 point specified, followed by a four-grid-point relaxation zone. From the outer domain the
18 model is one-way nested down to the 3-km domain covering all of Svalbard (Fig. 1). Within
19 both domains the model is allowed to freely evolve (i.e. no nudging or re-initialization), and
20 sea surface temperatures and sea ice fractions are prescribed based on the OSTIA dataset
21 (Donlon et al., 2012). The physical parameterization options in WRF follow Aas et al. (2015)
22 with the exceptions of the boundary layer and surface layer parameterizations, the vertical
23 model resolution, and the use of explicit 6th order horizontal advection diffusion, which are
24 selected following Collier et al. (2013). In addition, we use the newer NoahMP land surface
25 scheme to simulate surface conditions and fluxes at non-glaciated grid cells, as it includes
26 improved snow physics and multiple layers in the snowpack over the original Noah scheme
27 (Niu et al., 2011). All three model domains use the same vertical resolution (40 eta layers up
28 to a model top of 25 hPa) and physical parameterizations, with the exception of the cumulus
29 convection scheme that is only employed in the outer (9-km) domain.

30 The simulation was performed as one transient 10-year simulation, with a one-day spin up for
31 the atmosphere. The glacier grid points were initialized with output from an earlier simulation
32 with another version of the WRF-CMB model. This did not include results valid for 2003, so

1 a representative year (2007) was used for initialization. Although not accurate, this was
2 considered far more realistic than the default uniform initialization. The one-month sensitivity
3 simulation with 9-km, 3-km and 1-km grid spacings has been performed as an isolated
4 additional simulation with initialization directly from ERA-Interim to avoid problems with
5 different spin up times for the different domains.

6 **2.2 The glacier CMB model**

7 The land surface schemes in WRF have become more advanced in terms of representing snow
8 processes in the recent years, but still only simulate a few snow layers (up to three for
9 NoahMP). They therefore have limitations when it comes to simulating the development of
10 deep multiyear snow packs in the accumulation area of Svalbard glaciers, as well as
11 realistically representing different glacier facies (snow, firn and ice) during the ablation
12 season. We therefore used a modified version of the glacier climatic mass balance (CMB)
13 model of Mölg et al. (2008, 2009) to simulate glacier grid cells. The CMB model uses near
14 surface temperature, humidity, pressure, winds, as well as incoming radiation and
15 precipitation as input from WRF, and computes the column specific mass balance from solid
16 precipitation, surface and subsurface melt, refreezing, and liquid water storage in the
17 snowpack, and surface vapor fluxes. The model solves the surface energy balance (SEB) to
18 determine the energy available for surface melt, and resolves the glacier subsurface down to a
19 user defined depth (here 20 m divided into 17 vertical layers). For glacier grid cells, the CMB
20 model updates surface mass and energy fluxes in the WRF model, as well as surface
21 temperature, roughness, and albedo, resulting in a two-way coupled model system (WRF-
22 CMB). Further information about the interactive coupling between the CMB model and WRF
23 is given by Collier et al. (2013, 2015).

24 We make two adjustments to the CMB model to improve its suitability for Svalbard
25 conditions. First, the albedo scheme (originally based on Oerlemans and Knap, 1998) has
26 been modified to include a separate value for firn albedo (in addition to the standard
27 categories of fresh snow, old snow, and ice). Firn is defined here as snow remaining from the
28 last summer. Secondly, we introduce different aging models for snow (which determines the
29 transition from fresh to old snow) for melting and sub-melting temperatures, by multiplying
30 the snow aging parameter by a factor (*warmfact*, Table 1) when skin temperatures are at the
31 melting point. The various albedo parameters (Table 1) have been selected based on
32 observations at Austfonna, and thereafter adjusted to improve the simulated summer mass

1 balance compared to in situ observations during one test year (2005-2006; see also Sect.
2 6.1.1).

3 **2.3 Validation data and sites**

4 Table 2 provides an overview of the datasets used for model evaluation. We selected four
5 glaciers, described in more detail below, all of which have mass balance stake measurements
6 at six or more locations, covering all or most years in our study period. The selected sites
7 represent different conditions in terms of glacier geometry, geographical location, local
8 meteorology, altitudinal range, and spatial extent (Fig. 1). Annual measurements of stake
9 heights above the snow surface, snow depth, and density yield specific values of summer and
10 winter mass balance (b_s and b_w), which are combined to give the specific net mass balance, b_n
11 (SMB) for each balance year (i.e. between two consecutive end-of-summers).

12 GPR measurements of snow accumulation along several transects across the Austfonna ice
13 cap were made each spring in the period 2004-2013. Snow water equivalent (SWE) values are
14 derived from the radar estimated snow depths multiplied by snow density determined at
15 several snow pits, as described in more detail by Dunse et al. (2009).

16 Meteorological records at hourly resolution are available from two AWSs, one at Austfonna
17 and one on Kongsvegen. Both datasets contain some data gaps. We extract hourly
18 measurements of air temperature (~2 m) and radiation (incoming and outgoing short- and
19 long-wave), to calculate daily means, excluding days with incomplete records. Albedo is
20 calculated as the ratio of the outgoing (SW_{out}) to incoming (SW_{in}) shortwave radiation,
21 excluding observations outside the range [0.15, 0.95] or with $SW_{in} < 10 \text{ W m}^{-2}$. We estimate
22 daily mean albedo using the five hourly observations closest to solar noon, to minimize the
23 effect of low solar angle with associated large variations in measured albedo (Schuler et al.,
24 2013).

25 A geodetic mass-balance estimate from repeat satellite altimetry for the period 2003-2008
26 (Moholdt et al., 2010) serves as an independent validation of the surface height changes due
27 to climatic mass balance processes. However, it should be kept in mind that the geodetic
28 mass-balance reflects both climatic and dynamic mass balance, i.e. it includes mass transfer
29 from higher to lower elevations and losses due to calving at marine termini. We use the
30 regional mean values between 2003 and 2008 according to Fig. 1.

1 2.3.1 Austfonna ice cap, Northeast Svalbard

2 The Austfonna ice cap in the northeastern part of Svalbard (centered at 79.7° N, 24.0° E) is
3 the largest ice cap of the archipelago. It covers an area of 7800 km² and has a simple dome-
4 shaped topography, rising from sea level up to an elevation of ~800 m a.s.l. (Moholdt and
5 Kääb 2012). The recent CMB of Austfonna was nearly in balance (Moholdt et al., 2010), yet
6 the ice cap was losing mass due to calving and retreat of the marine margin (Dowdeswell et
7 al., 2008). Snow accumulation is spatially and temporally heterogeneous and asymmetrical
8 across the ice cap, with amounts in the southeast being double the amounts in the northwest
9 and large interannual variability along all profiles (Pinglot et al., 1999; Taurisano et al., 2007;
10 Dunse et al., 2009).

11 Since spring 2004, field measurements have been performed annually by the University of
12 Oslo and the Norwegian Polar Institute. Available data include records from about 20 mass
13 balance stakes, annually repeated GPR and kinematic GNSS (Global Navigation Satellite
14 System) profiling across the ice cap, and snow pit investigations of snow depth and density
15 (Taurisano et al., 2007; Dunse et al., 2009). In the present study we compare GPR-derived
16 winter accumulation with the corresponding WRF-CMB results, averaging all available in situ
17 measurements within a particular WRF-CMB grid cell (Sect. 3.3).

18 Etonbreen is located at the western part of Austfonna, with six stakes, and an AWS operated
19 since 2004. The AWS is located at 22°25'12'' E, 79°43'48''N and 370 m a.s.l., just below the
20 mean equilibrium line altitude (ELA) of ~400m (Schuler et al., 2013).

21 2.3.2 Kongsvegen and Holtedahlfonna, Northwest Spitsbergen

22 Kongsvegen (78.8°N, 13.0°E) and Holtedahlfonna (79.0°N, 13.5°E) are both located near Ny-
23 Ålesund, in northwest Spitsbergen.

24 Kongsvegen is a ~100 km², ~27-km long valley glacier extending from an ice divide at ~800
25 m a.s.l. down to sea level. Outflow at its marine terminus is restricted by its fast-flowing
26 neighbor Kronebreen, with which Kongsvegen shares a small fraction of the calving front.

27 The Norwegian Polar Institute has measured winter and summer mass balance at nine stakes
28 since 1986 (Hagen et al., 2003; Nuth et al., 2012; Karner et al., 2013). Kongsvegen is a surge-
29 type glacier, currently in its quiescent phase, since the last surge around 1948. Observed
30 elevation changes are dominated by the SMB (Melvold and Hagen 1998).

1 North of Kongsvegen is Holvedahlfonna, the upper catchment of the Holvedahlfonna-
2 Kronebreen glacier system, whose total area is $\sim 390 \text{ km}^2$, and which extends up to an
3 elevation of $\sim 1400 \text{ m a.s.l.}$ SMB has been studied on Holvedahlfonna since spring 2003, using
4 ten mass-balance stakes.

5 Stakes at both glaciers are measured in nearly all years in spring and at the end-of-summer,
6 typically in early September. During the last two decades, the SMB of both glaciers has
7 changed from close to zero to increasingly negative values (Kohler et al., 2007; Nuth et al.,
8 2012). Since spring 2000, an AWS has been operated on Kongsvegen, at 78.76°N , 13.16°E at
9 537 m a.s.l. , close to the ELA (Karner et al., 2013).

10 2.3.3 Hansbreen, Southern Spitsbergen

11 Hansbreen (77.1°N , 15.6°E) is located in the southern part of Spitsbergen, and covers an area
12 of $\sim 56 \text{ km}^2$. It is a 15 km long valley glacier, extending from its $\sim 1.5 \text{ km}$ wide active calving
13 front in Isbjornhamna, Hornsund, up to an ice divide at $\sim 490 \text{ m a.s.l.}$ The Hansbreen system
14 consists of the main trunk glacier and 4 tributary glaciers on the west side (Grabiec et al.,
15 2011). SMB on Hansbreen has been studied since 1989 when 11 mass balance stakes were
16 deployed along centerline of the glacier. Since 2005 these stakes are measured on a weekly
17 basis in ablation zone and on a monthly basis in accumulation area (Grabiec et al., 2012).

18 Snow accumulation on Hansbreen is highly variable. Earlier studies show that there is a
19 strong asymmetry between eastern and western side of the glacier. Minimal snow
20 accumulation is observed in southern part of the tongue and along eastern side of the glacier.
21 On the east side, the glacier is bordered by the massif of Sofiekammen, which forms an
22 orographic barrier for advecting air masses. Therefore, a foehn effect is widely observed
23 during strong easterly winds, causing deflation of snow and redeposition towards the western
24 side of the glacier (Grabiec et al., 2006).

25 2.4 Comparison methods

26 We compare our model results with AWS (Sect. 3.1) and stake (Sect. 3.2) data using the
27 WRF-CMB grid point nearest to each data point. All stakes on a glacier are compared with
28 the corresponding grid cells to yield information both about mean values as well as gradients
29 along the glacier. The ELA (also Sect. 3.2) is calculated by linear interpolation of the two
30 stakes or grid cells with the least positive and negative mass balance. When all stakes or grid

1 cells have the same sign, we use the maximum and minimum value to extrapolate to the ELA.
2 Note that the CMB simulated by WRF-CMB also includes internal refreezing below the last
3 summer surface (LSS), which is not captured by the stake SMB.

4

5 **3 Model validation**

6 In the following sections, we assess the model performance by comparing the simulated SEB
7 and temperature with the AWS data (Sect. 3.1); the CMB at the four glaciers with stake
8 measurements (Sect. 3.2); the winter accumulation at Austfonna with GPR measurements
9 (Sect. 3.3); and, finally, the simulated regional height changes over the first five years of the
10 study period with the altimetry data (Sect. 3.4). All model results in this section are from the
11 3-km domain.

12 **3.1 Weather stations**

13 The AWSs provide key information about the conditions at the glacier surface throughout the
14 year, and therefore permit a detailed evaluation of important aspects of the model. Table 3
15 compares simulated and observed air temperature, radiation fluxes, and albedo at Kongsvegen
16 and Etonbreen. Note that the model grid points are 44 m and 29 m lower than the station
17 heights at these two locations, respectively. At Kongsvegen the simulated temperature
18 compares very well with observations, with a bias of 0.19 °C and correlation of daily mean
19 values of 0.98. At Etonbreen the simulated temperatures are somewhat too low (-1.9 °C), but
20 with a similar correlation (0.96). The radiation components also show better agreement at
21 Kongsvegen than at Etonbreen. At Kongsvegen, biases ranging from 0.3 W m⁻² (outgoing
22 longwave, LW_{out}) to -6.9 W m⁻² (incoming longwave, LW_{in}), whereas the radiation biases at
23 Etonbreen vary from -4.0 (LW_{out}) to -13 W m⁻² (SW_{in}). There is also a noticeable albedo bias
24 of -0.10 at Etonbreen, compared to only -0.05 at Kongsvegen.

25 A more detailed comparison of simulated and observed albedo from the summers of 2008 and
26 2013 is shown in Fig. 2, along with simulated solid and liquid precipitation. Overall, the
27 model simulates well both the magnitude and temporal changes in albedo. The close
28 connection between simulated solid precipitation events and observed albedo increase
29 indicates that the model adequately captures both the timing and phase of the summer
30 precipitation. The simulated albedo response to solid precipitation is also similar to
31 measurements, except at Etonbreen in 2013. Here the model does not simulate a large enough

1 increase in albedo after snow events, which might indicate that the model is not sensitive
2 enough to small amounts of snow on ice (i.e. too large depth scale in Table 1), or
3 underestimates precipitation or its frozen fraction on these occasions. Additionally, the model
4 underestimates snow albedo during much of the summer in 2008, and at Etonbreen also
5 simulates some periods with blue ice. While the observations show a very slow decrease in
6 albedo over this summer, the modeled albedo quickly drops to values below 0.7. This could
7 be related to the almost complete lack of rain events during the summer of 2008. In 2013, on
8 the other hand, the model simulates numerous and large rain events during the summer, which
9 seems to coincide with observed drops in albedo. This suggests that snow wetness needs to be
10 accounted for in the albedo parameterization to realistically simulate snow albedo on
11 Svalbard, and that the snow aging parameters used here (Table 1) are more appropriate for
12 wet rather than dry summer conditions.

13 Altogether, the model seems to reasonably reproduce the local conditions at the AWS
14 stations. Individual radiation biases are found, which are likely to impact the quality of the
15 CMB estimations negatively. However, this is a known challenge in the Arctic, where
16 atmospheric models often show significant biases in key cloud properties (Morrison et al.,
17 2009).

18 **3.2 Stakes**

19 Fig. 3 shows mean annual (b_n), winter (b_w), and summer (b_s) CMB at each stake over the
20 study period. Overall, the model reproduces the mean observed mass balances well, including
21 differences in mean values between the four glaciers and the gradients at each glacier. The
22 main exception is the winter balance at Hansbreen, which is considerably underestimated by
23 the model (see Sect. 4). Hansbreen also shows large variations along the glacier, both in b_s
24 and b_w , which the model is not able to reproduce.

25 Looking at individual years, the model correctly identifies the years 2004 and 2008 as having
26 anomalously low and high mass balance, respectively (Fig. 3, stippled lines). The agreement,
27 however, is not as good for these two years as for the mean values.

28 To look further at temporal variations, we compare modeled ELA to that derived from stake
29 measurements (Fig. 4). In general there is good agreement both in terms of ELA as well as
30 inter-annual variability, with the exception again being Hansbreen. Here the model strongly
31 overestimates ELA, in accordance with the underestimation of b_w (Fig. 3). However, at this

1 glacier, the observed mass balance – elevation relationship shows considerable non-linearity,
2 with the observations indicating zero b_n at several elevations during some years, rendering
3 ambiguous ELA estimates. For the other three glaciers the model simulates ELA well,
4 including the large difference between Kongsvegen and Holtedahlfonna, which are located
5 close to each other (Fig. 1).

6 **3.3 GPR-derived snow profiles**

7 To evaluate the winter-mass balance simulated by WRF-CMB, we compare simulated
8 precipitation across Austfonna between early September and early May with observations of
9 snow accumulation by GPR. The results from May 2004 and May 2006 (Fig. 5) demonstrate
10 the large inter-annual variability in the total amount of snow, with 2004 and 2006
11 representing a low (Fig. 5a) and high (Fig. 5c) accumulation year, respectively. WRF-CMB
12 captures the spatial pattern and total amount of snow very well, with average biases of about
13 2% and 6% and mean absolute errors (MAEs) of 47 and 67 mm w.e. yr^{-1} in 2004 and 2006
14 respectively. Local differences, for example an overestimation of snow within the ablation
15 area towards the lower end of the western profile in both years (Fig. 5b,d) may partly be
16 explained by wind erosion, which is not represented in the model. The model also tends to
17 slightly underestimate snow accumulation in the summit area, which again could be related to
18 wind redistribution of snow, or by a negative elevation bias of the WRF-CMB DEM which is
19 on average ~20-50m lower than the average position of the GPR measurements.

20 **3.4 Satellite altimetry**

21 We perform a regional evaluation of the simulations by comparing surface height changes
22 with those measured by satellite altimetry in the period 2003-2008 (Moholdt et al., 2010).
23 Note that measured height changes are also a result of glacier dynamics (although the retreat
24 or advance of the calving front was not accounted for). The model, however, does not include
25 any glacier dynamics and the numbers are therefore not directly comparable. Still, both model
26 and satellite data show Austfonna and northeast Spitsbergen to be the only regions with
27 positive surface height change during these years, and northwest Spitsbergen as the region
28 with the largest surface lowering (Table 4). The other three regions all show moderate
29 lowering in both estimates. The model therefore seems to capture regional differences very
30 well during this period. The mass loss from calving flux has been estimated to be 6.75 km³
31 yr^{-1} (w.e.) for the years 2000-2006 (Blaszczyk et al., 2009), which corresponds to an

1 additional lowering of about 0.2 m yr^{-1} . This suggests that the model in general simulates too
2 much surface lowering in this period. However the time periods are different and the estimate
3 of Moholdt et al. (2010) does not include the effect of retreat or advance of the calving front.
4 One must therefore still be cautious when comparing these numbers.

5 Together, these results show that the model captures the spatial and temporal variability in
6 CMB across Svalbard well, with mean values in fair agreement with observations. The largest
7 model errors are found at Hansbreen, which has both the largest cross-glacier variability in
8 accumulation and as a relatively steep accumulation gradient, such that the stake
9 measurements may not correlate as well to the model as at other sites with a greater degree of
10 spatial homogeneity. This raises the question about the sensitivity of model resolution in
11 relation to capturing the main topographic features.

12

13 **4 Sensitivity to model resolution**

14 Svalbard topography is relatively rugged, with fjords, tundra, glaciers and mountains all
15 found in close proximity to each other. Dynamical downscaling requires a discrete
16 representation of the topography and has therefore limited spatial resolution, which
17 potentially can be insufficient to resolve a number of small-scale processes. In this section, we
18 investigate the sensitivity of simulated CMB to model resolution by comparing results from
19 the 9-km and 3-km domains for the entire model period. We then evaluate precipitation
20 amounts and distribution in a separate simulation with 9-km, 3-km and 1-km grid spacings
21 (hereafter R9, R3 and R1) of the month of October 2007, which was among the wettest
22 months in the 10-year period, with a number of smaller and larger precipitation events.

23 Fig. 6 shows the mean annual CMB in R9 and R3 over the entire period. When averaged
24 across all of Svalbard, the difference is relatively small ($\sim 30 \text{ mm w.e. yr}^{-1}$). On a regional
25 scale, however, differences are more substantial, with the southeastern islands (BE region in
26 Fig. 1) having almost $100 \text{ mm w.e. yr}^{-1}$ more negative mass balance in R9 than in R3. The
27 modest difference found when averaging across the entire archipelago is therefore at least
28 partly due to compensating regional differences. On the local scale, differences are even
29 more pronounced. The lack of small glaciers in R9 gives large ice-free areas compared with
30 R3 (e.g. in much of central Spitsbergen). The CMB gradient is also often larger in R3 than
31 R9, as higher maximum and lower minimum values are resolved, which is likely key for long-
32 term model simulations, where geometry adjustments of glaciers are considered.

1 The level of detail resolved also plays an important role in model evaluation, especially when
2 comparing to in situ point measurements. Fig. 7 shows the terrain height in the three regions
3 with stake measurements for R9, R3 and R1. Here we see new topographic features and a
4 more detailed coastline emerging with each increase in resolution. In R9 the topographic
5 gradients along the glaciers with stakes are mostly too low, and many stakes maps on to the
6 same grid cell. Conversely, in R3 most stakes maps on to individual grid cells and the
7 altitudinal range is in better agreement with the stakes (see also Fig. 3). Still, there are distinct
8 topographic features around these four glaciers that only emerge in R1. For example, the
9 model represents Hansbreen, Kongsvegen and the upper part of Holtedahlfonna as valley
10 glaciers only at this resolution. The simulated precipitation from October 2007 (Fig. 8) also
11 shows distinct differences between the three resolutions. At Etonbreen, the shape of the
12 precipitation curve along the glacier is very different in R9 compared with R3 and R1. The
13 other three glaciers show more linear increases in precipitation with altitude during this month
14 at all three resolutions. Still the precipitation amount varies and mainly increases with higher
15 resolution, with local differences of up to about 50 mm (25 %), at Hansbreen (~300 m a.s.l.).

16 We therefore conclude that increasing resolution from 9-km to 3-km grid spacings is
17 important for simulating precipitation and CMB on local and regional scales, as well as for
18 reliable comparison with in situ point measurements. Increasing the resolution further to 1-km
19 grid spacing seems to have a smaller effect on the four glaciers investigated, although the
20 precipitation amount is further increased. Model resolution might therefore explain some of
21 the negative model bias in b_w (cf. Fig. 3). However, resolution alone does not explain the
22 large b_w bias at Hansbreen. Instead it is likely that processes like wind drift and snow
23 redistribution are important for the accumulation pattern on this glacier. These processes
24 likely also affect the accumulation at the other glaciers, however their influence is largely
25 unconstrained.

26

27 **5 Climatic mass balance**

28 We now turn to simulated annual and seasonal CMB results for Svalbard and the different
29 sub-regions (Fig. 1). Consistent with previous studies (e.g. Hagen et al., 2003; Lang et al.,
30 2015b) we find large inter-annual variation in CMB (Fig. 9 and Table 5), which precludes
31 trend analysis on the timescales considered in this study. Likewise, our mean mass balance
32 value of $-257 \text{ mm w.e. yr}^{-1}$ depends on the model period considered; five-year mean values

1 vary from $-313 \text{ mm w.e. yr}^{-1}$ (2009-2013) and $-27 \text{ mm w.e. yr}^{-1}$ (2006-2010). Multiplied with
2 a glacier area of $34\,000 \text{ km}^2$ (Nuth et al., 2013), these values correspond to a mean annual
3 mass loss of 8.7 Gt, 11 Gt, or 0.92 Gt, respectively.

4 Comparing the two seasons reveals that summer mass balance varies about twice as much as
5 winter mass balance (Fig. 9), indicating that ablation processes vary more from year to year
6 than winter accumulation. This is confirmed from the annual mass fluxes shown in Fig. 10b,
7 with solid precipitation showing much less variability than surface melting. Melting is in turn
8 largely a result of the radiation imbalance during the summer months (JJA; Fig. 10a), which
9 on average accounts for about 80 % of the net energy to the surface during these months.
10 However, years with anomalously large melting (especially 2004 and 2013) are characterized
11 by much larger than normal sensible and latent heat fluxes at the surface. As these fluxes
12 indicate warmer and moister air in the atmosphere relative to the glacier surface, the melting
13 anomalies likely result from advection of warm air from outside the region, as was also found
14 by Lang et al. (2015b) for the year 2013.

15 For the individual regions we find large differences in simulated CMB that persists
16 throughout the whole period (Fig. 9; right axis). Most noticeably the northeastern regions
17 (AF, VF and NE) show less negative summer balance than the Svalbard average and mostly
18 lower than average winter accumulation. The regions with high winter accumulation in the
19 south and east correspond to the regions with the lowest ELA reported by Hagen et al. (2003;
20 see also mean annual precipitation and ELA estimates in the Supplement).

21

22 **6 Discussion**

23 **6.1 Comparison with earlier studies**

24 We will focus our comparison here with the two regional model studies that report
25 comparison with SMB or CMB measurements, namely DA12 and LA15b (Sect. 1). Both of
26 these studies compare their results with ice core measurements in accumulation areas (Pinglot
27 et al., 1999; Pinglot et al., 2001), although DA12 only includes accumulation and not melting
28 in their simulation. DA12 finds biases ranging from -240 to $130 \text{ mm w.e. y}^{-1}$ with a mean
29 absolute error close to $100 \text{ mm w.e. y}^{-1}$, whereas LA15b reports biases between -310 and 140
30 mm w.e. y^{-1} , with a MAE of $100 \text{ mm w.e. y}^{-1}$. Our simulation period does not cover these ice
31 core measurements so that a direct comparison is not possible. Still, the MAEs in winter

1 accumulation at Austfonna (Fig. 5) are 47 and 67 mm w.e. y^{-1} for 2004 and 2006 respectively.
2 At the stake locations, the simulated CMB (Fig. 3) is mostly within about 100 mm w.e. y^{-1} of
3 the observations, except at Hansbreen where it ranges from close to zero to about 1000 mm
4 w.e. y^{-1} . Our CMB results are therefore an improvement compared to DA12 and LA15b when
5 Hansbreen is ignored (where processes not represented in our model are believed to be
6 important).

7 The near surface temperature biases are in both DA12 and LA15b larger than ours. DA12
8 reports annual biases “less than 2 °C” for two stations, and “less than 6 °C” for the third
9 (Kongsvegen) and LA15 showed annual biases between -1.3 and -4.0 °C (all negative). We
10 only use data from the two AWSs on the glaciers here, with biases of 0.19 and -1.9 °C at
11 Kongsvegen and Etonbreen respectively. These biases span the two-year mean biases found
12 by Claremar et al. (2012), and are also similar to those found by Aas et al. (2015) for the year
13 2008-2009 (including also tundra sites), both using the WRF model.

14 Some of the improvement found in the present study can probably be attributed to the
15 increased model resolution. Both smaller elevation differences between stations and the
16 model grid cell and better resolved surrounding topography likely improved the results. We
17 also note here that our results do not cover the same time periods as DA12 and LA15b, so that
18 the quality of the boundary conditions might differ. However, LA15b reports relatively small
19 biases for ERA-Interim (between -1.95 and 2.24 °C) despite similar or larger elevation
20 differences and covering the same period as LA15b. Also, the large increase in resolution
21 from DA12 (25 km) to LA15b (10 km) is not accompanied with a clear improvement in the
22 mass balance simulation. It therefore seems clear that the WRF-CMB model with the setup
23 used here offers a real improvement over DA12 and LA15b.

24 **6.2 Model uncertainties**

25 In the following section we discuss the main uncertainties in the model results, starting with
26 the atmospheric forcing, before discussing the representation of albedo, turbulent fluxes and
27 sub-surface processes in the CMB model. Although we recognize that the observations have
28 uncertainties and limitations, it is beyond the scope of this study to go into those here.

1 6.2.1 Atmospheric forcing

2 The quality of any CMB simulation depends largely on the atmospheric forcing used. In this
3 study we have used a coupled atmosphere-glacier model in which the atmospheric component
4 (WRF) has been well tested for this region. It has been shown to produce temperatures that
5 are in good agreement with observations, and relatively small biases in energy fluxes on
6 annual time scales, although they can differ significantly on seasonal and shorter time scales
7 (Aas et al., 2015). Deviations from observations can come both from insufficient
8 representation of processes within the WRF model and from errors in the boundary conditions
9 (here ERA-Interim and OSTIA). However, comparison with weather stations (Sect. 3.1) and
10 the results from Aas et al. (2015) show that there is good agreement with observations for the
11 atmospheric part, compared to similar studies (Claremar et al., 2012; DA12; LA15b).

12 6.2.2 Albedo

13 The albedo parameterization in the CMB model uses a set of parameters that likely varies
14 considerably for different locations but is treated as spatially invariant. Initially, these
15 parameters were set based on data from the AWS at Austfonna, where we had the longest
16 series of radiation data. This, however, gave too little summer ablation in general, and these
17 parameters were therefore instead tuned to give summer mass balance values in line with
18 observations based on a set of sensitivity simulations of the year 2005-2006 with the 9-km
19 grid spacing domain. The resulting values (Table 1) are similar to those used by van Pelt et al.
20 (2012). With the complex model system used here we cannot perform a set of simulations at
21 the full resolution and time period, but only acknowledge that these values are uncertain, and
22 should ideally vary across the region. Greuell et al. (2007) found MODIS ice albedo values at
23 different glaciers across Svalbard between 0.44 (Etonbreen) and 0.13 (Lisbethbreen), which
24 also explains why our initial values from Etonbreen gave too little summer ablation in
25 general. A large step forward for CMB modelling of this region would therefore be to include
26 spatially varying albedo parameters based on satellite measurements. Including snow wetness
27 could also offer improvements for simulation of changes in snow albedo with time (see
28 section 3.1).

29 6.2.3 Atmospheric stability

30 We have seen that the sensible and latent heat fluxes are an important part of the SEB during
31 the ablation season (Sect. 5). However, the simulation of these fluxes in stable conditions is a

1 major challenge subject to ongoing research (e.g. Holtslag et al., 2013). In our setup of the
2 CMB model, we use a stability correction based on the bulk Richardson number (Braithwaite,
3 1995). Conway and Cullen (2013) found that this correction gives too low fluxes during
4 stable conditions and low wind speeds at a New Zealand Southern Alps glacier, with
5 simulated turbulent fluxes close to zero when observations showed values between 50-100 W
6 m⁻². Based on their results, and to avoid runaway cooling of the glacier surface during stable
7 conditions in the winter, we limited the reduction in the turbulent fluxes in stable conditions
8 to 30%, consistent with previous studies (Martin and Lejeune, 1998; Giesen et al., 2009;
9 Collier et al., 2015).. Due to these issues, and since they are not measured at the study
10 glaciers, these fluxes also contribute to the overall model uncertainty.

11 6.2.4 Sub-surface processes

12 As can be seen from Fig. 10b, the sub-surface components (refreezing, superimposed ice,
13 subsurface melting, and change in liquid water content) contribute considerably to the total
14 simulated CMB. An important simplification in the CMB model is the use of a bulk snow
15 density, as it is not intended for detailed snowpack studies. For the highest areas on Austfonna
16 and Northeast Spitsbergen, where the simulated snow and firn accumulation reaches values of
17 14 m during the simulation, this simplification is likely inappropriate. In addition, the CMB
18 model currently calculates superimposed ice as a specified fraction of the internal refreezing
19 of liquid water. Modeling this process is challenging, even with a vertically resolved
20 treatment of snow density. Thus, while the inclusion of the sub-surface processes likely offers
21 an important step forward compared to only simulating the surface mass balance, the accuracy
22 of these sub-surface processes in the model needs to be improved.

23

24 7 Conclusions

25 In this study, we simulated the CMB of the Svalbard archipelago with a coupled atmosphere-
26 glacier model, for the period 2003 to 2013 with 9-km and 3-km grid spacings, as well as with
27 1-km grid spacing for a shorter period. The results have been compared with extensive
28 observational data from weather stations, mass balance stakes, ground penetrating radar and
29 satellite altimetry. Our main findings are:

- 30 - The WRF-CMB model with 3-km grid spacing and the configuration used here
31 reproduces observed CMB on Svalbard very well, from local to regional scales.

- 1 - We confirm the need for high spatial resolution (1-5 km grid spacing) to realistically
2 simulate CMB at glacier scale, as suggested by Day et al. (2012). The results from 3-
3 km and 1-km grid spacings show distinct features at local scales that are not present at
4 9-km, and mean CMB at regional scale differed by up to ~ 100 mm w.e. yr^{-1} between
5 the 3-km and 9-km simulations.
- 6 - Large variations in CMB on small spatial scales reduce the representativeness of
7 individual point measurements when compared with grid cells larger than 1-5 km.
- 8 - We find large year-to-year variability in average CMB on Svalbard during our
9 simulation period, which can be mainly attributed to variations in melting. The largest
10 component in the summer surface energy balance driving this melting is the radiation
11 imbalance, even though temperature dependent latent and sensible heat fluxes also
12 contribute to much of the year-to-year variability, especially during the years with
13 anomalously large mass loss. More research is however needed to better understand
14 the drivers of this variability.

15 For the first time, this study presents results from dynamical downscaling of Svalbard CMB at
16 the resolution suggested by Day et al. (2012). In addition, we have utilized a large number of
17 observations on different spatial scales to get a robust evaluation of model performance,
18 thereby representing a considerable step forward in the pursuit of reliable simulations of the
19 CMB on Svalbard. Further improvements to several aspects of the WRF-CMB would be
20 desirable for this region, including using spatially variable albedo parameters and improved
21 representation of sub-surface processes. Still the WRF-CMB model – which has not
22 previously been validated for Arctic conditions – has here been shown to be an appropriate
23 tool for studying Svalbard CMB.

24

25 **Acknowledgements**

26 We thank two anonymous reviewers for valuable comments and suggestions to the original
27 manuscript and V. Radić for acting as Editor. This study was mainly carried out as a part of
28 the CryoMet project funded by the Norwegian Research Council (NFR 214465).
29 Additionally, it was partially supported within statutory activities No 3841/E-41/S/2015 of the
30 Ministry of Science and Higher Education of Poland, as well as well as being supported by

- 1 Nordic Center of Excellence eSTICC (eScience Tools for Investigating Climate Change at
- 2 high northern latitudes) funded by Nordforsk (grant 57001).
- 3

1 References

- 2 Aas, K. S., Berntsen, T. K., Boike, J., Eitzelmueller, B., Kristjansson, J. E., Maturilli, M.,
3 Schuler, T. V., Stordal, F., and Westermann, S.: A Comparison between Simulated and
4 Observed Surface Energy Balance at the Svalbard Archipelago, *Journal of Applied*
5 *Meteorology and Climatology*, 54, 1102-1119, 2015.
- 6 Blaszczyk, M., Jania, J. A., and Hagen, J. O.: Tidewater glaciers of Svalbard: Recent changes
7 and estimates of calving fluxes, *Pol. Polar Res*, 30, 85-142, 2009.
- 8 Braithwaite, R. J.: Aerodynamic stability and turbulent sensible heat flux over a melting ice
9 surface, the Greenland ice sheet, *J. Glaciol.*, 41, 562–571, 1995.
- 10 Claremar, B., Obleitner, F., Reijmer, C., Pohjola, V., Waxegard, A., Karner, F., and
11 Rutgersson, A.: Applying a Mesoscale Atmospheric Model to Svalbard Glaciers, *Adv.*
12 *Meteorol.*, 2012, 321649, doi: 10.1155/2012/321649, 2012. 2012.
- 13 Cogley, J.G., Hock, R., Rasmussen, L.A., Arendt, A.A., Bauder, A., Braithwaite, R.J.,
14 Jansson, P., Kaser, G., Möller, M., Nicholson, L., and Zemp, M.: Glossary of Glacier
15 Mass Balance and Related Terms, IHP-VII Technical Documents in Hydrology No. 86,
16 IACS Contribution No. 2, UNESCO-IHP, Paris. 2011
- 17 Collier, E., Maussion, F., Nicholson, L. I., Mölg, T., Immerzeel, W. W., and Bush, A. B. G.:
18 Impact of debris cover on glacier ablation and atmosphere–glacier feedbacks in the
19 Karakoram, *The Cryosphere*, 9, 1617-1632, 2015.
- 20 Collier, E., Mölg, T., Maussion, F., Scherer, D., Mayer, C., and Bush, A. B. G.: High-
21 resolution interactive modelling of the mountain glacier-atmosphere interface: an
22 application over the Karakoram, *Cryosphere*, 7, 779-795, 2013.
- 23 Conway, J. P. and Cullen, N. J.: Constraining turbulent heat flux parameterization over a
24 temperate maritime glacier in New Zealand, *Ann. Glaciol.*, 54, 41-51, 2013.
- 25 Day, J. J., Bamber, J. L., Valdes, P. J., and Kohler, J.: The impact of a seasonally ice free
26 Arctic Ocean on the temperature, precipitation and surface mass balance of Svalbard,
27 *Cryosphere*, 6, 35-50, 2012.
- 28 Dee, D. P., Uppala, S. M., Simmons, A. J., Berrisford, P., Poli, P., Kobayashi, S., Andrae, U.,
29 Balmaseda, M. A., Balsamo, G., Bauer, P., Bechtold, P., Beljaars, A. C. M., van de Berg,
30 L., Bidlot, J., Bormann, N., Delsol, C., Dragani, R., Fuentes, M., Geer, A. J.,
31 Haimberger, L., Healy, S. B., Hersbach, H., Holm, E. V., Isaksen, L., Kallberg, P.,
32 Koehler, M., Matricardi, M., McNally, A. P., Monge-Sanz, B. M., Morcrette, J. J., Park,
33 B. K., Peubey, C., de Rosnay, P., Tavolato, C., Thepaut, J. N., and Vitart, F.: The ERA-
34 Interim reanalysis: configuration and performance of the data assimilation system,
35 *Quarterly Journal of the Royal Meteorological Society*, 137, 553-597, 2011.

- 1 Donlon, C. J., Martin, M., Stark, J., Roberts-Jones, J., Fiedler, E., and Wimmer, W.: The
2 Operational Sea Surface Temperature and Sea Ice Analysis (OSTIA) system, *Remote*
3 *Sens. Environ.*, 116, 140-158, 2012.
- 4 Dowdeswell, J. A., Benham, T. J., Strozzi, T., and Hagen, J. O.: Iceberg calving flux and
5 mass balance of the Austfonna ice cap on Nordaustlandet, Svalbard, *J. Geophys. Res.-*
6 *Earth*, 113, F03022, doi:10.1029/2007JF000905, 2008.
- 7 Dunse, T., Schuler, T. V., Hagen, J. O., Eiken, T., Brandt, O., and Hogda, K. A.: Recent
8 fluctuations in the extent of the firn area of Austfonna, Svalbard, inferred from GPR,
9 *Ann. Glaciol.*, 50, 155-162, 2009.
- 10 Førland, E. J., Benestad, R., Hanssen-Bauer, I., Haugen, J. E., and Skaugen, T. E.:
11 Temperature and Precipitation Development at Svalbard 1900-2100, *Adv. Meteorol.*,
12 2011, 893790, doi: 10.1155/2011/893790, 2011. 2011.
- 13 Giesen, R., Andreassen, L., Van den Broeke, M., and Oerlemans, J.: Comparison of the
14 meteorology and surface energy balance at Storbreen and Midtdalsbreen, two glaciers in
15 southern Norway, *The Cryosphere*, 3, 57-74, 2009. Grabiec, M., Jania, J., Puczko, D.,
16 Kolondra, L., and Budzik, T.: Surface and bed morphology of Hansbreen, a tidewater
17 glacier in Spitsbergen, *Polish Polar Research*, 33, 111-138, 2012.
- 18 Grabiec, M., Leszkiewicz, J., Głowacki, P., and Jania, J.: Distribution of snow accumulation
19 on some glaciers of Spitsbergen. *Polish Polar Research*, 27, 309-326, 2006.
- 20 Grabiec, M., Puczko, D., Budzik, T., and Gajek, G.: Snow distribution patterns on Svalbard
21 glaciers derived from radio-echo soundings. *Polish Polar Research*, 32, 393-421, 2011.
- 22 Greuell, W., Kohler, J., Obleitner, F., Glowacki, P., Melvold, K., Bernsen, E., and Oerlemans,
23 J.: Assessment of interannual variations in the surface mass balance of 18 Svalbard
24 glaciers from the Moderate Resolution Imaging Spectroradiometer/Terra albedo product,
25 *Journal of Geophysical Research-Atmospheres*, 112, D07105,
26 doi:10.1029/2006JD007245, 2007.
- 27 Hagen, J. O., Melvold, K., Pinglot, F., and Dowdeswell, J. A.: On the net mass balance of the
28 glaciers and ice caps in Svalbard, *Norwegian Arctic, Arct. Antarct. Alp. Res.*, 35, 264-
29 270, 2003.
- 30 Holtslag, A. A. M., Svensson, G., Baas, P., Basu, S., Beare, B., Beljaars, A. C. M., Bosveld,
31 F. C., Cuxart, J., Lindvall, J., Steeneveld, G. J., Tjernstrom, M., and Van de Wiel, B. J.
32 H.: STABLE ATMOSPHERIC BOUNDARY LAYERS AND DIURNAL CYCLES
33 Challenges for Weather and Climate Models, *Bulletin of the American Meteorological*
34 *Society*, 94, 1691-1706, 2013.
- 35 IPCC, van Oldenborgh, G.J., Collins, M., Arblaster, J., Christensen, J.H., Marotzke, J.,
36 Power, S.B., Rummukainen, M. and Zhou, T. (eds.): Annex I: Atlas of Global and
37 Regional Climate Projections Supplementary Material RCP8.5, in: *Climate Change*
38 *2013: The Physical Science Basis. Contribution of Working Group I to the Fifth*
39 *Assessment Report of the Intergovernmental Panel on Climate Change*, edited by:

- 1 Stocker, T. F., Qin, D., Plattner, G.-K., Tignor, M., Allen, S. K., Boschung, J., Nauels,
2 A., Xia, Y., Bex, V., and Midgley, P. M., available at: www.climatechange2013.org and
3 www.ipcc.ch (last access: 15 January 2015), AISM-1–AISM-159, 2013.
- 4 Karner, F., Obleitner, F., Krismer, T., Kohler, J., and Greuell, W.: A decade of energy and
5 mass balance investigations on the glacier Kongsvegen, Svalbard, *Journal of*
6 *Geophysical Research-Atmospheres*, 118, 3986-4000, 2013.
- 7 Kilpeläinen, T., Vihma, T., Manninen, M., Sjoblom, A., Jakobson, E., Palo, T., and Maturilli,
8 M.: Modelling the vertical structure of the atmospheric boundary layer over Arctic fjords
9 in Svalbard, *Quarterly Journal of the Royal Meteorological Society*, 138, 1867-1883,
10 2012.
- 11 Kilpeläinen, T., Vihma, T., and Olafsson, H.: Modelling of spatial variability and topographic
12 effects over Arctic fjords in Svalbard, *Tellus Series a-Dynamic Meteorology and*
13 *Oceanography*, 63, 223-237, 2011.
- 14 Kohler, J., James, T. D., Murray, T., Nuth, C., Brandt, O., Barrand, N. E., Aas, H. F., and
15 Luckman, A.: Acceleration in thinning rate on western Svalbard glaciers, *Geophysical*
16 *Research Letters*, 34, 5, L18502, doi:10.1029/2007GL030681, 2007.
- 17 Lang, C., Fettweis, X., and Erpicum, M.: Future climate and surface mass balance of Svalbard
18 glaciers in an RCP8.5 climate scenario: a study with the regional climate model MAR
19 forced by MIROC5, *Cryosphere*, 9, 945-956, 2015a.
- 20 Lang, C., Fettweis, X., and Erpicum, M.: Stable climate and surface mass balance in Svalbard
21 over 1979-2013 despite the Arctic warming, *Cryosphere*, 9, 83-101, 2015b.
- 22 Martin, E. and Lejeune, Y.: Turbulent fluxes above the snow surface, *Ann. Glaciol.*, 26, 179-
23 183, 1998.
- 24 Martin-Espanol, A., Navarro, F. J., Otero, J., Lapazaran, J. J., and Blaszczyk, M.: Estimate of
25 the total volume of Svalbard glaciers, and their potential contribution to sea-level rise,
26 using new regionally based scaling relationships, *Journal of Glaciology*, 61, 29-41, 2015.
- 27 Marzeion, B., Jarosch, A. H., and Hofer, M.: Past and future sea-level change from the
28 surface mass balance of glaciers, *Cryosphere*, 6, 1295-1322, 2012.
- 29 Marzeion, B., Leclercq, P. W., Cogley, J. G., and Jarosch, A. H.: Brief Communication:
30 Global glacier mass loss reconstructions during the 20th century are consistent, *The*
31 *Cryosphere Discuss.*, 9, 3807-3820, 2015.
- 32 Matsuo, K. and Heki, K.: Current Ice Loss in Small Glacier Systems of the Arctic Islands
33 (Iceland, Svalbard, and the Russian High Arctic) from Satellite Gravimetry, *Terrestrial*
34 *Atmospheric and Oceanic Sciences*, 24, 657-670, 2013.
- 35 Melvold, K. and Hagen, J. O.: Evolution of a surge-type glacier in its quiescent phase:
36 Kongsvegen, Spitsbergen, 1964-95, *Journal of Glaciology*, 44, 394-404, 1998.

- 1 Mémin, A., Rogister, Y., Hinderer, J., Omang, O. C., and Luck, B.: Secular gravity variation
2 at Svalbard (Norway) from ground observations and GRACE satellite data, *Geophys. J.*
3 *Int.*, 184, 1119–1130, doi:10.1111/j.1365-246X.2010.04922.x, 2011.
- 4 Moholdt, G. and Käab, A.: A new DEM of the Austfonna ice cap by combining differential
5 SAR interferometry with ICESat laser altimetry, *Polar Res.*, 31, L18502,
6 doi:10.1029/2007GL030681, 2012.
- 7 Moholdt, G., Nuth, C., Hagen, J. O., and Kohler, J.: Recent elevation changes of Svalbard
8 glaciers derived from ICESat laser altimetry, *Remote Sens. Environ.*, 114, 2756-2767,
9 2010.
- 10 Mölg, T., Cullen, N. J., Hardy, D. R., Kaser, G., and Klok, L.: Mass balance of a slope glacier
11 on Kilimanjaro and its sensitivity to climate, *International Journal of Climatology*, 28,
12 881-892, 2008.
- 13 Mölg, T., Cullen, N. J., Hardy, D. R., Winkler, M., and Kaser, G.: Quantifying Climate
14 Change in the Tropical Midtroposphere over East Africa from Glacier Shrinkage on
15 Kilimanjaro, *J. Clim.*, 22, 4162-4181, 2009.
- 16 Morrison, H., McCoy, R. B., Klein, S. A., Xie, S. C., Luo, Y. L., Avramov, A., Chen, M. X.,
17 Cole, J. N. S., Falk, M., Foster, M. J., Del Genio, A. D., Harrington, J. Y., Hoose, C.,
18 Khairoutdinov, M. F., Larson, V. E., Liu, X. H., McFarquhar, G. M., Poellot, M. R., von
19 Salzen, K., Shipway, B. J., Shupe, M. D., Sud, Y. C., Turner, D. D., Veron, D. E.,
20 Walker, G. K., Wang, Z. E., Wolf, A. B., Xu, K. M., Yang, F. L., and Zhang, G.:
21 Intercomparison of model simulations of mixed-phase clouds observed during the ARM
22 Mixed-Phase Arctic Cloud Experiment. II: Multilayer cloud, *Quarterly Journal of the*
23 *Royal Meteorological Society*, 135, 1003-1019, 2009.
- 24 Niu, G.-Y., Yang, Z.-L., Mitchell, K. E., Chen, F., Ek, M. B., Barlage, M., Kumar, A.,
25 Manning, K., Niyogi, D., Rosero, E., Tewari, M., and Xia, Y.: The community Noah
26 land surface model with multiparameterization options (Noah-MP): 1. Model description
27 and evaluation with local-scale measurements, *Journal of Geophysical Research-*
28 *Atmospheres*, 116, D12109, doi:10.1029/2010JD015139, 2011.
- 29 Nuth, C., Kohler, J., König, M., von Deschanden, A., Hagen, J. O., Käab, A., Moholdt, G.,
30 and Pettersson, R.: Decadal changes from a multi-temporal glacier inventory of
31 Svalbard, *Cryosphere*, 7, 1603-1621, 2013.
- 32 Nuth, C., Moholdt, G., Kohler, J., Hagen, J. O., and Käab, A.: Svalbard glacier elevation
33 changes and contribution to sea level rise, *J. Geophys. Res.*, 115, F01008,
34 doi:10.1029/2008JF001223, 2010.
- 35 Nuth, C., Schuler, T. V., Kohler, J., Altena, B., and Hagen, J. O.: Estimating the long-term
36 calving flux of Kronebreen, Svalbard, from geodetic elevation changes and mass-balance
37 modelling, *Journal of Glaciology*, 58, 119-133, 2012.
- 38 Oerlemans, J. and Knap, W. H.: A 1 year record of global radiation and albedo in the ablation
39 zone of Morteratschgletscher, Switzerland, *Journal of Glaciology*, 44, 231-238, 1998.

- 1 Østby, T. I., Schuler, T. V., Hagen, J. O., Hock, R., and Reijmer, L. H.: Parameter
2 uncertainty, refreezing and surface energy balance modelling at Austfonna ice cap,
3 Svalbard, 2004-08, *Ann. Glaciol.*, 54, 229-240, 2013.
- 4 Pinglot, J. F., Hagen, J. O., Melvold, K., Eiken, T., and Vincent, C.: A mean net accumulation
5 pattern derived from radioactive layers and radar soundings on Austfonna,
6 Nordaustlandet, Svalbard, *Journal of Glaciology*, 47, 555-566, 2001.
- 7 Pinglot, J. F., Pourchet, M., Lefauconnier, B., Hagen, J. O., Isaksson, E., Vaikmae, R., and
8 Kamiyama, K.: Accumulation in Svalbard glaciers deduced from ice cores with nuclear
9 tests and Chernobyl reference layers, *Polar Res.*, 18, 315-321, 1999.
- 10 Schuler, T. V., Dunse, T., Østby, T. I., and Hagen, J. O.: Meteorological conditions on an
11 Arctic ice cap—8 years of automatic weather station data from Austfonna, Svalbard,
12 *International Journal of Climatology*, 34, 2047–2058, doi: 10.1002/joc.3821, 2013.
- 13 Skamarock, W. C. and Klemp, J. B.: A time-split nonhydrostatic atmospheric model for
14 weather research and forecasting applications, *J. Comput. Phys.*, 227, 3465–3485, 2008.
- 15 Taurisano, A., Schuler, T. V., Hagen, J. O., Eiken, T., Loe, E., Melvold, K., and Kohler, J.:
16 The distribution of snow accumulation across the Austfonna ice cap, Svalbard: direct
17 measurements and modelling, *Polar Res.*, 26, 7-13, 2007.
- 18 van Pelt, W. J. J., Oerlemans, J., Reijmer, C. H., Pohjola, V. A., Pettersson, R., and van
19 Angelen, J. H.: Simulating melt, runoff and refreezing on Nordenskiöldbreen, Svalbard,
20 using a coupled snow and energy balance model, *Cryosphere*, 6, 641-659, 2012.
- 21 Wouters, B., Chambers, D., and Schrama, E. J. O.: GRACE observes small-scale mass loss in
22 Greenland, *Geophys. Res. Lett.*, 35, L20501, doi:10.1029/2008GL034816, 2008.
- 23

1

Parameter	Value
Ice albedo	0.33
Firn albedo (new)	0.50
Old snow albedo	0.63
Fresh snow albedo	0.87
Time scale	15 days
<i>warmfact</i> (new)	5
Depth scale*	3.0 cm

2

Table 1. Albedo parameters used in the CMB model.

3

* Refers to physical snow depth.

4

1

Region	Data	Time period	References
Austfonna, including Etonbreen	AWS	Hourly, since 2004, some data gaps	Schuler et al., 2013
	MB stakes	Annually, since 2004	Moholdt et al., 2010; Østby et al., 2013
	GPR	Annually, since 2004	Taurisano et al., 2007 ; Dunse et al., 2009
	Snow pits	Annually, since 2004	Dunse et al., 2009
Kongsvegen	AWS	Hourly, since 2004, some data gaps	Karner et al., 2013
	MB stakes	Biannually, since 1986	Nuth et al., 2012
Holtedahlfonna	MB stakes	Biannually, since 2003	Nuth et al., 2012
Hansbreen	MB stakes	Biannually, since 1988 (two years missing). Weekly/monthly since 2005.	Grabiec et al., 2012
Svalbard	Satellite altimetry		Moholdt et al., 2010

2

Table 2. Description of observations

3

1

	Etonbreen			Kongsvegen		
	Bias	MAE	Corr.	Bias	MAE	Corr.
T_2 (°C)	-1.9	2.4	0.96	0.19	1.4	0.98
SW_{in} ($W\ m^{-2}$)	-13	43	0.81	-0.28	21	0.96
SW_{out} ($W\ m^{-2}$)	-10	17	0.93	-6.7	19	0.96
LW_{in} ($W\ m^{-2}$)	-12	25	0.82	-6.9	17	0.89
LW_{out} ($W\ m^{-2}$)	-3.8	11	0.95	0.32	6.1	0.97
Albedo	-0.10	0.12	0.73	-0.05	0.08	0.80

2 Table 3. Bias, mean absolute error (MAE) and correlation between simulated and observed
3 daily mean temperature, radiation and albedo at Etonbreen and Kongsvegen.

4

1

	WRF-CMB	Moholdt et al., (2010)
Northwest Spitsbergen	-0.44	-0.54
Northeast Spitsbergen	0.02	0.06
South Spitsbergen	-0.33	-0.15
Barenstøya/Edgeøya	-0.35	-0.17
Vestfonna	-0.34	-0.16
Austfonna	0.05	0.11
Svalbard	-0.18	-0.11

2

Table 4. 2003-2008 mean surface elevation change rates (m yr^{-1}) from WRF-CMB and

3

Moholdt et al., 2010. The Svalbard mean value from Moholdt et al. (2010) used here is the

4

mean of the regions included here (Fig. 1) weighted by area.

5

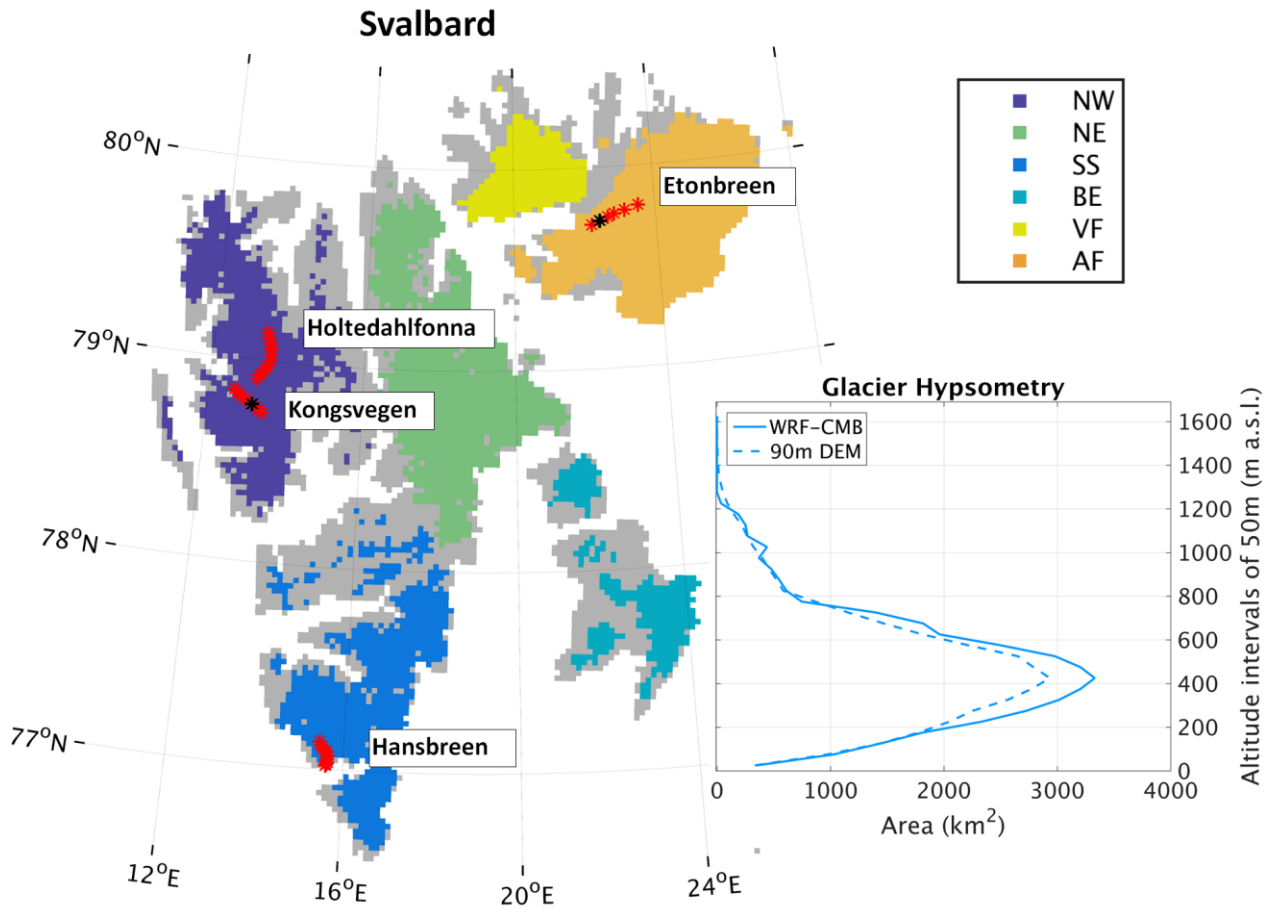
1

	Svalbard		NW		NE		SS		BE		VF		AF	
	Mean	SD	Mean	SD	Mean	SD	Mean	SD	Mean	SD	Mean	SD	Mean	SD
SPR	639	107	588	107	647	118	774	138	703	113	491	91	586	111
REF	141	21	126	23	151	23	143	21	125	18	112	23	152	27
SUI	60	9.2	54	10	65	10	61	9.0	54	7.7	48	10	65	12
DEP	51	7.9	50	7.1	45	6.5	64	11	64	13	47	8.7	44	6.8
MLT	-1000	262	-1090	243	-837	250	-1350	315	-1260	398	-876	271	-776	256
SUM	-124	27	-147	38	-111	26	-148	33	-132	36	-114	32	-98	26
SBL	-26	2.6	-28	3.3	-27	2.3	-23	2.6	-22	3.1	-26	3.2	-28	3.2
DLW	4.0	12	3.1	10.3	5.8	16.8	2.2	10.7	1	6.4	2.7	10.2	5.5	19
CMB	-257	358	-439	376	-62	347	-481	464	-465	484	-314	337	-49	323

2 Table 5. Mean annual CMB fluxes (mm w.e. yr⁻¹) and standard deviations (SD) for Svalbard
3 and each sub-region in Figure 1. SPR: solid precipitation, REF: refreeze, SUI: superimposed
4 ice, DEP: deposition, MLT: surface melt, SUM: sub-surface melt, SLB: sublimation, DLW:
5 change in snow liquid water.

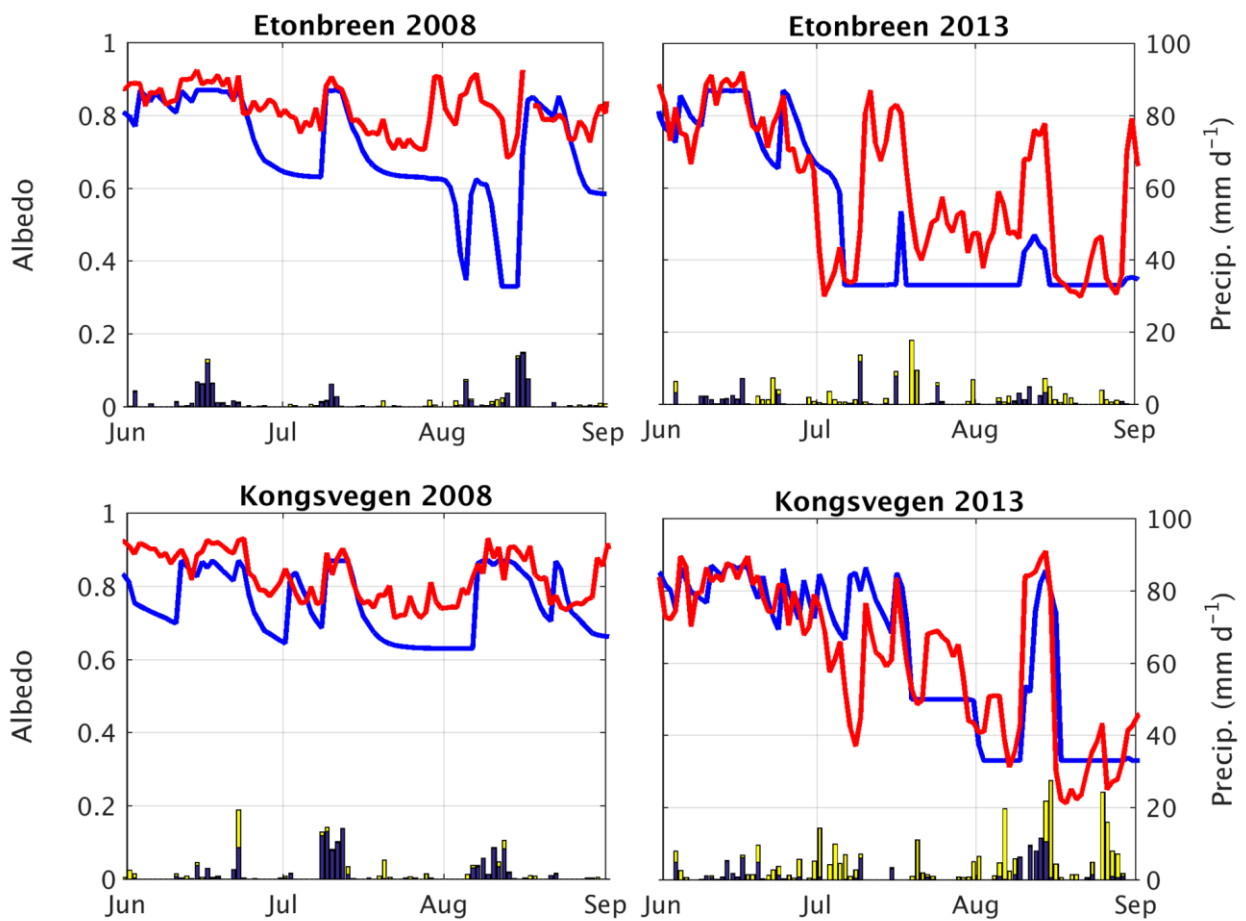
6

1



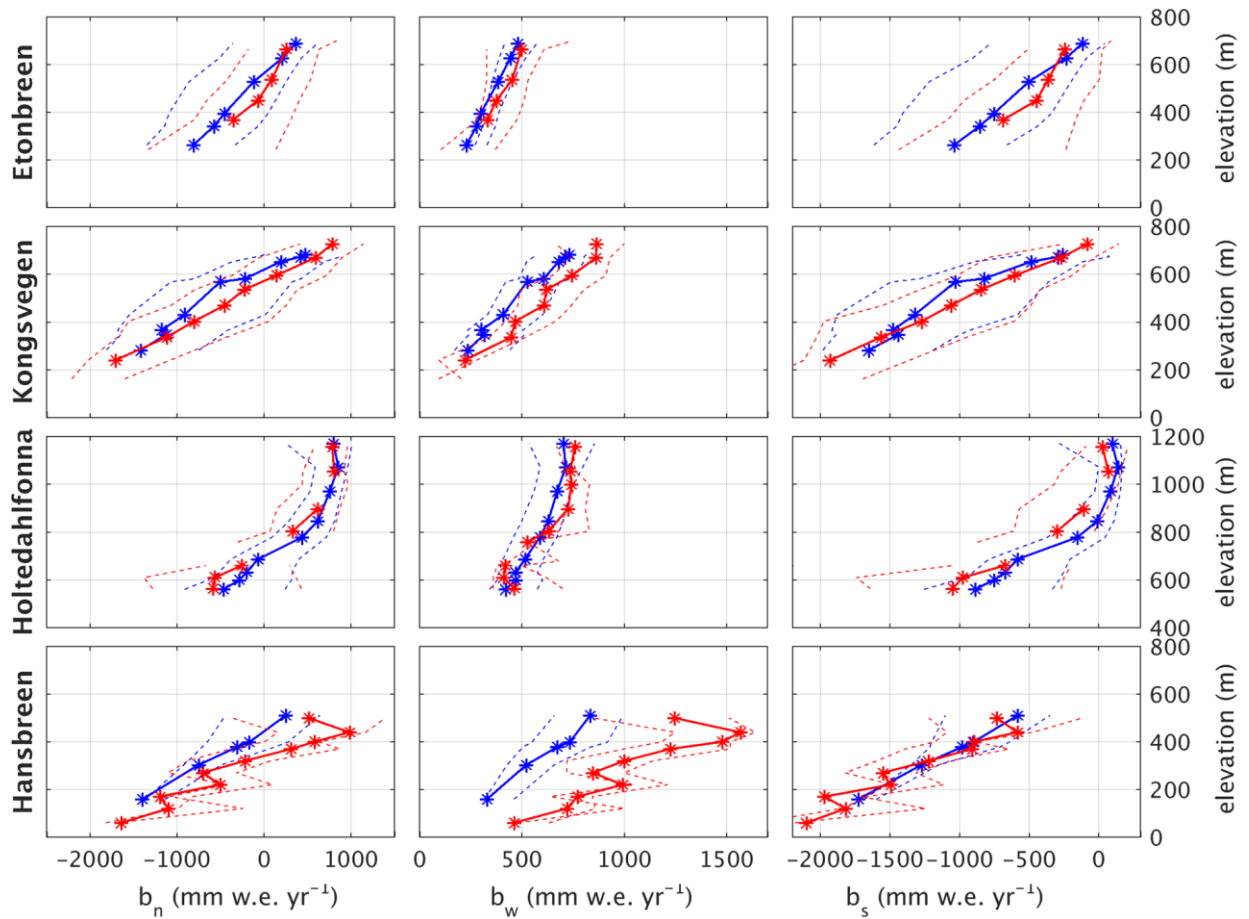
2

3 Figure 1. Main figure: Land areas in the 3-km model domain. Colors indicate glacier grid
4 cells in different sub-regions and gray indicate non-glacier land grid cells. Stake and AWS
5 locations at the four main validation glaciers are shown as red * and black *, respectively.
6 NW: northwestern Spitsbergen, NE: northeastern Spitsbergen, SS: southern Spitsbergen, BE:
7 Barentsøya and Edgeøya, VF: Vestfonna and AF: Austfonna. Overlay figure: Glacier
8 hypsometry from 3-km model domain compared with 90m DEM (Nuth et al., 2013).



1

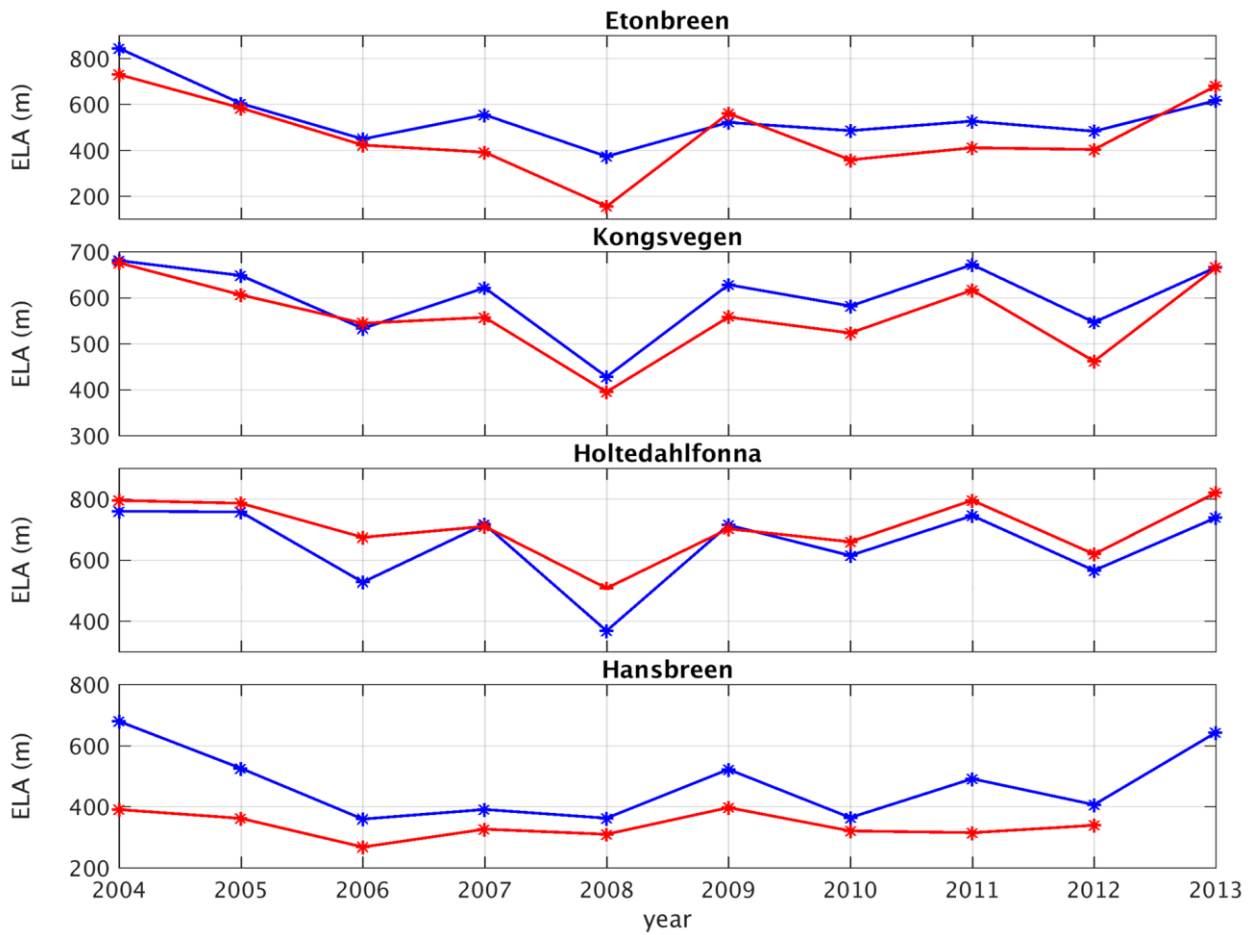
2 Figure 2. Simulated (blue) and observed (red) albedo at Etonbreen and Kongsvegen for the
 3 summers 2008 and 2013, with simulated solid (blue) and liquid (yellow) precipitation
 4 indicated as bars.



1

2 Figure 3. Simulated (blue) and observed (red) annual, winter and summer mass balance at the
 3 four main validation glaciers. The 10-year mean is indicated by solid lines and the years 2004
 4 and 2008 (negative and positive anomaly, respectively) are shown as dashed lines. Stars
 5 indicate elevation of individual stakes (red) or grid cells (blue).

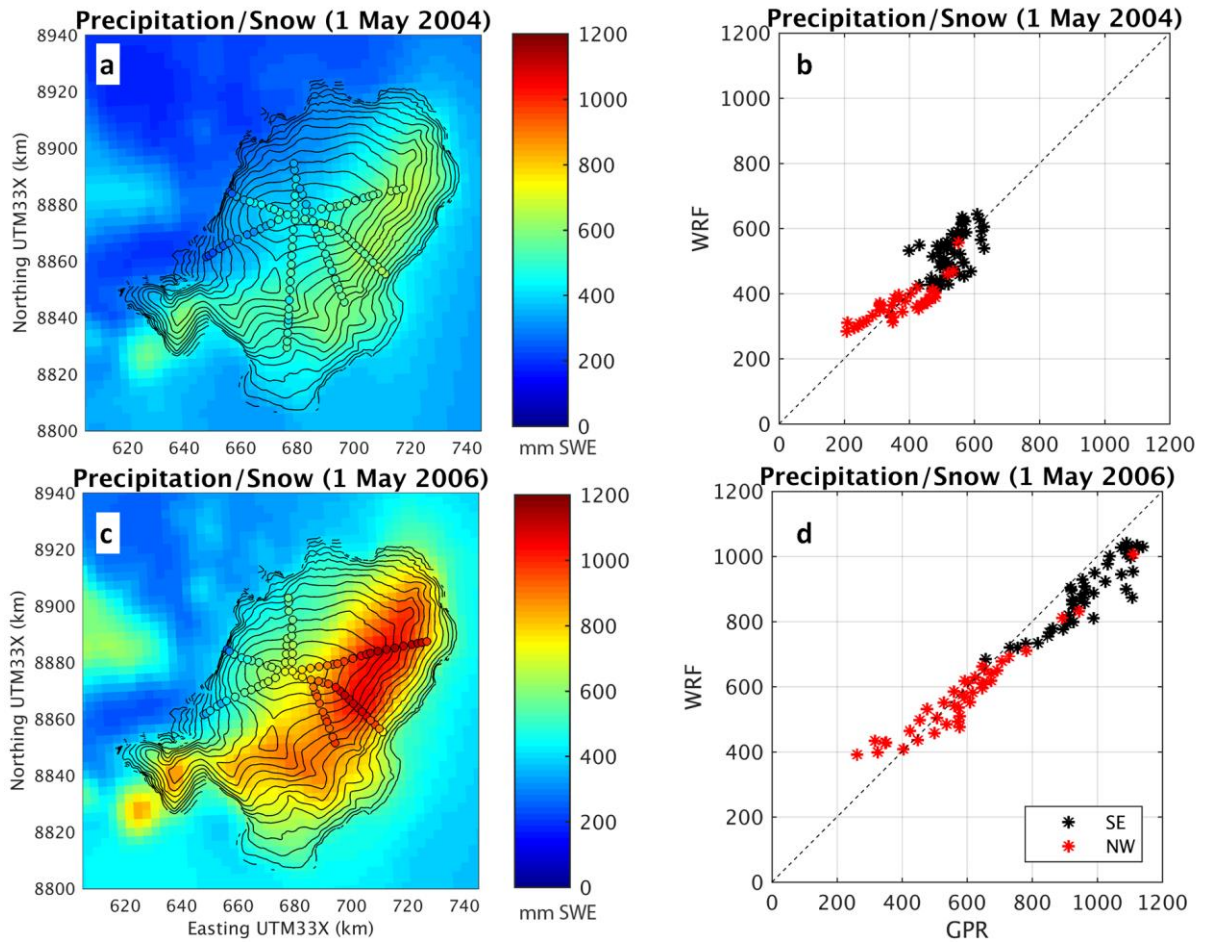
6



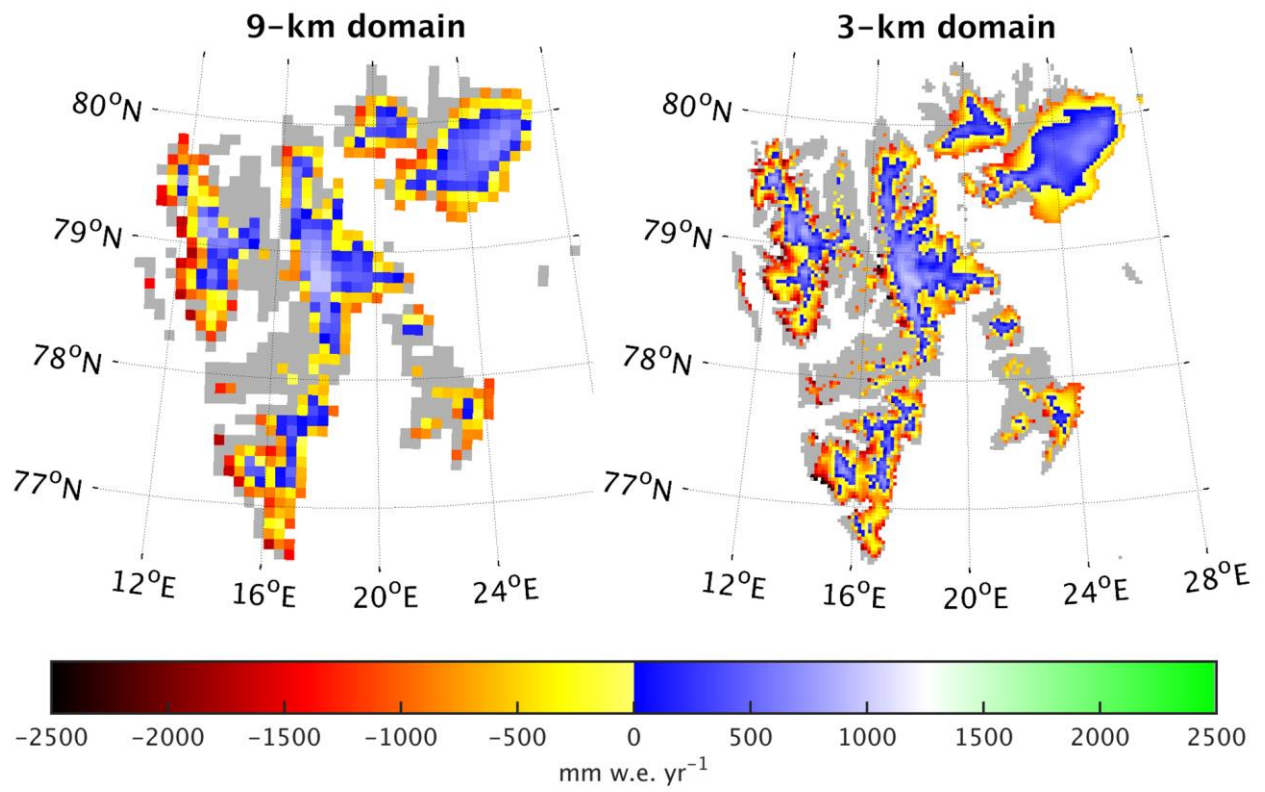
1

2 Figure 4. Estimated ELA from WRF-CMB (blue) and stakes (red) at the four main validation
 3 glaciers.

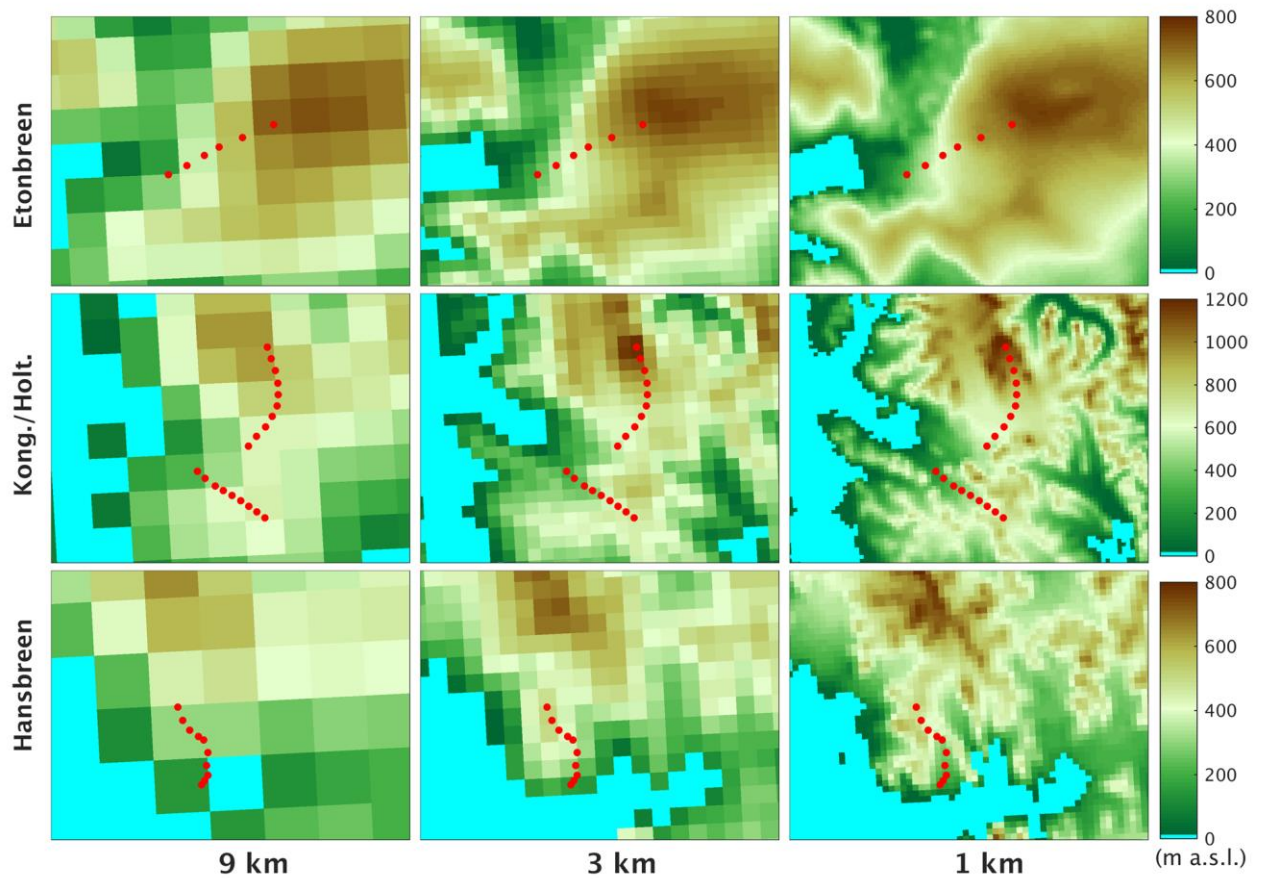
4



1
 2 Figure 5. a) Simulated and GPR-derived winter accumulation at Austfonna 1 May 2004. b)
 3 Scatterplot of data from GPR locations in a). Red dots show points located northwest of
 4 summit, and black dots show points located southeast of summit. c) Same as a) for 1 May
 5 2006. d) Same as b) for 1 May 2006.
 6



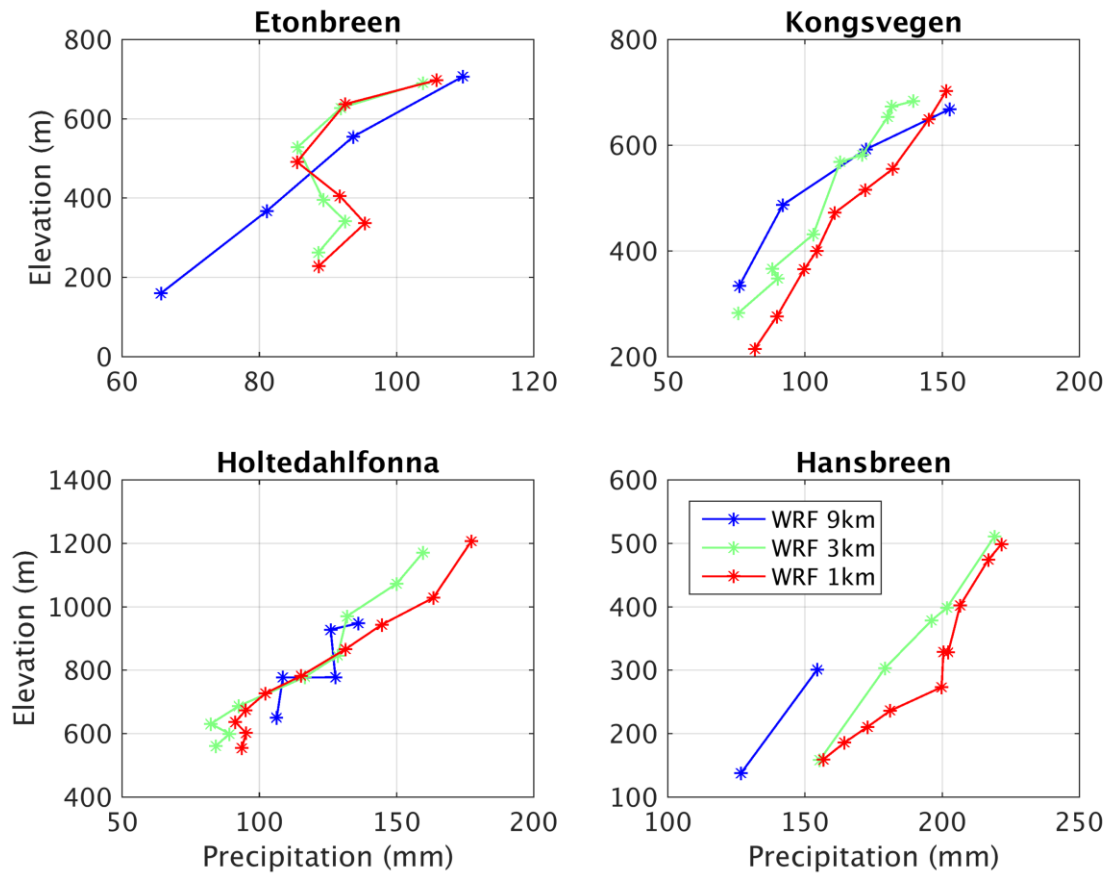
1
 2 Figure 6. Mean annual CMB (mm w.e. yr⁻¹) from 2003 to 2013 simulated with 9-km (left)
 3 and 3-km (right) grid spacings.
 4



1

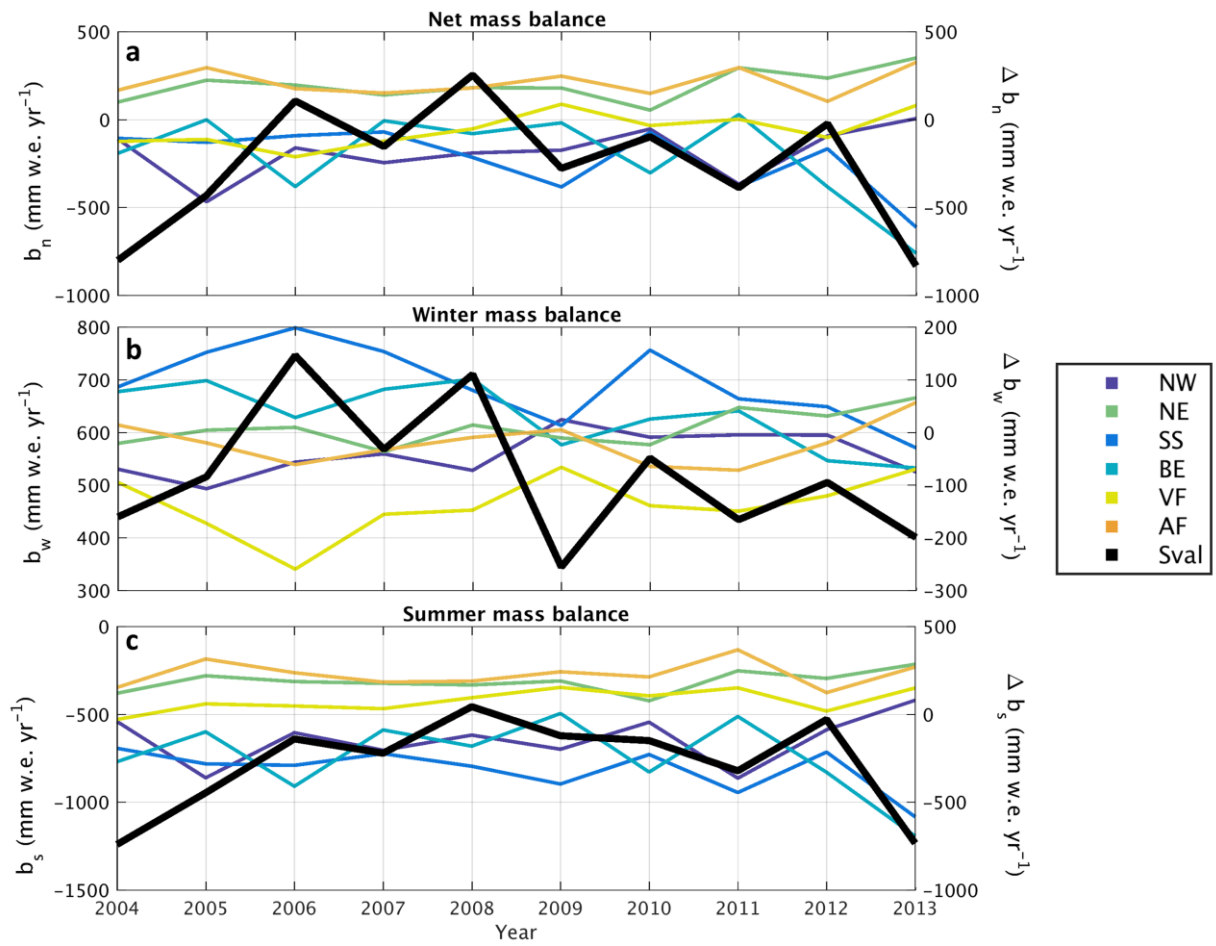
2 Figure 7. Model topography at 9-km, 3-km and 1-km grid spacings around Etonbreen (top),
 3 Kongsvegen and Holvedahlfonna (middle) and Hansbreen (bottom). Red dots indicate stake
 4 locations.

5



1
 2 Figure 8. Precipitation during October 2007 at stake locations with 9-km (blue), 3-km (green)
 3 and 1-km (red) grid spacing.

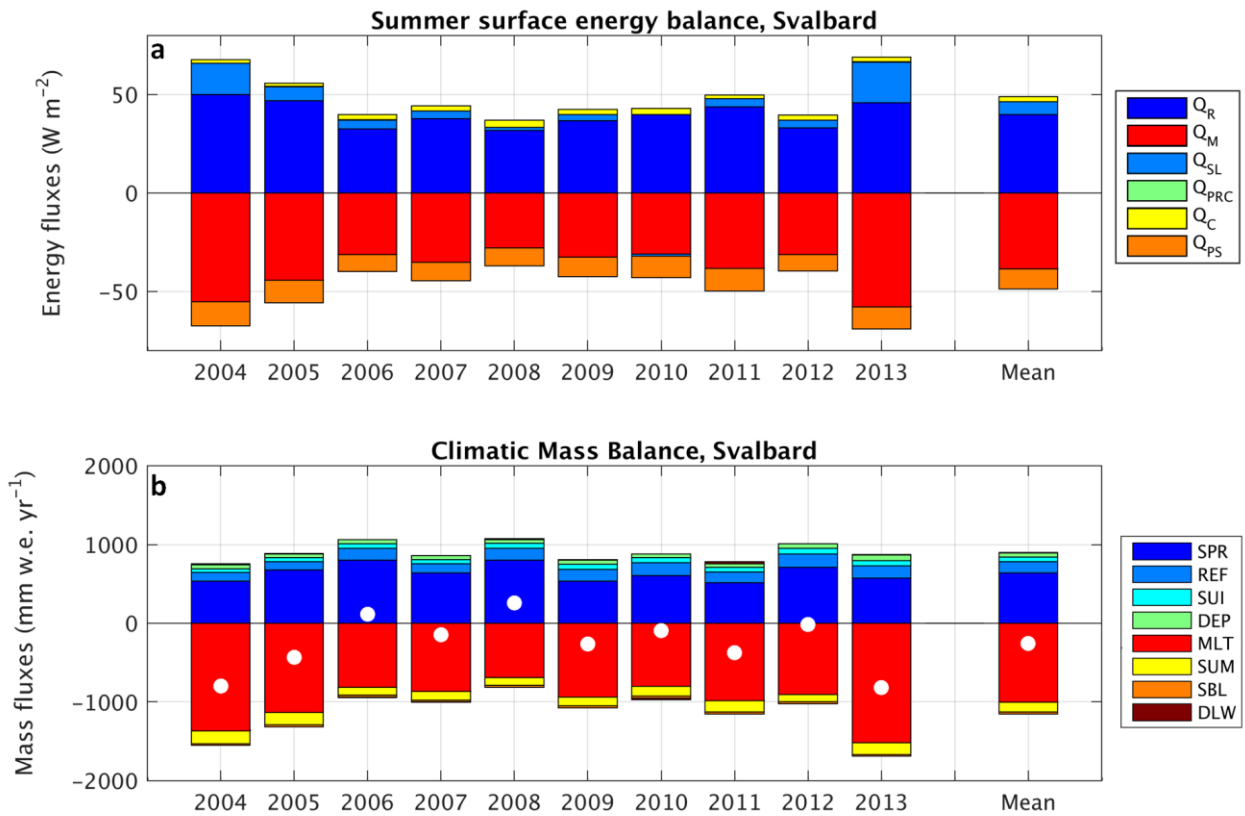
4



1

2 Figure 9. (a) annual mean mass balance (m w.e. yr⁻¹) for Svalbard (black, left y-axis) and
 3 regional deviations (colors, right y-axis). (b) same as (a) but for winter mass balance (Sept. to
 4 April). (c) same as for (a) but for summer mass balance (May to August).

5



1
 2 Figure 10. (a) Mean summer (JJA) surface energy balance fluxes. Q_R : net radiation, Q_M : melt
 3 energy, Q_{SL} : sensible and latent heat flux, Q_{PRC} : heat from precipitation, Q_C : ice heat flux and
 4 Q_{PS} : penetrating solar radiation. (b) Annual mass fluxes averaged over Svalbard. SPR: solid
 5 precipitation, REF: refreeze, SUI: superimposed ice, DEP: deposition, MLT: surface melt,
 6 SUM: sub-surface melt, SBL: sublimation, DLW: change in snow liquid water. The resulting
 7 CMB is indicated by white dots.